

Two-Photon Absorption and Excited-State Energy-Transfer Properties of a New Multibranching Molecule

S.-J. Chung, T.-C. Lin, K.-S. Kim, G. S. He, J. Swiatkiewicz, P. N. Prasad,*
G. A. Baker, and F. V. Bright

Photonics Research Laboratory, Institute for Lasers, Photonics, and Biophotonics,
Department of Chemistry, University at Buffalo, The State University of New York,
Buffalo, New York 14260-3000

Received February 21, 2001. Revised Manuscript Received July 9, 2001

This paper presents a molecular design for a two-photon absorbing structure, which contains a two-dimensional molecular architecture with four arms and one bridging unit, each of these segments having an extended π -conjugation and capable of producing two-photon absorption in different spectral ranges. Two chromophore units of a triphenylamine derivative dye, (*N,N*-di[4-(5-[4-*tert*-butylphenyl]-1,3,4-oxadiazol-2-yl)styryl]phenyl)amino)benzene, were linked with a π -conjugated di-2-thienylethenylene bridging unit to form a new multibranching compound, bis(5-[4-(*N,N*-di(4-[4-(5-(4-*tert*-butylphenyl)-1,3,4-oxadiazol-2-yl)styryl]phenyl)amino)styryl]thien-2-yl)ethenylene. Linear absorption spectra and luminescence spectra of the component and the multibranching chromophores revealed a hypochromic effect for the multibranching dye. A very effective energy transfer from the excited arm units to the π -conjugated bridging unit is observed. The two-photon cross-sections were measured using the femtosecond *Z*-scan technique at several excitation wavelengths in the 620–800 nm range. Comparing the nonlinear absorption coefficients observed for the constituent chromophore dyes with that for the multibranching compound, we found that the arm units make the dominant contribution to the two-photon absorption when the wavelength of excitation is longer than 720 nm.

Introduction

Pioneering work by Rentzepis^{1,2} in data storage and by Webb^{3,4} in microscopy early demonstrated the potential of the application of two-photon processes. Since then there has been considerable interest in the design, synthesis, and characterization of new organic chromophores and polymers with potentially large two-photon cross-sections for a variety of photonic applications. These photonic applications include optical power limiting,^{5,6} two-photon fluorescence imaging,^{3,7,8} two-photon photodynamic cancer therapy,^{9,10} and two-photon microfabrication.^{11,12}

A number of known chromophores promote the two-photon absorption (TPA) effect; however, the detailed structure–property relationships for the design criteria of new chromophores with large two-photon cross-

sections have been lacking. Recent reports^{13–19} from various groups show design strategies for efficient TPA molecules by a systematic investigation of chromophores with various electron-donor and electron-acceptor moieties, which are attached symmetrically or asymmetrically to a conjugated linker (π -center). The effects of varying the electron-donating or electron-accepting strength of end groups, introducing additional groups in the middle to vary the charge redistribution, and varying the effective conjugation length have been

- (1) Parthenopoulos, D. A.; Rentzepis, P. M. *Science* **1989**, *249*, 843.
- (2) Dvornikov, A. S.; Rentzepis, P. M. *Opt. Commun.* **1995**, *119*, 341.
- (3) Denk, W.; Strickler, J. H.; Webb, W. W. *Science* **1990**, *248*, 73.
- (4) Wu, En, S.; Strickler, J. H.; Harrell, W. R.; Webb, W. W. *SPIE Proc.* **1992**, *1674*, 776.
- (5) Fleitz, P. A.; Sutherland, R. A.; Strogkendl, F. P.; Larson, F. P.; Dalton, L. R. *SPIE Proc.* **1998**, *3472*, 91.
- (6) He, G. S.; Bhawalkar, J. D.; Zhao, C. F.; Prasad, P. N. *Appl. Phys. Lett.* **1995**, *67*, 2433.
- (7) Wang, X.; Krebs, L. J.; Al-Nuri, M.; Pudavar, H. E.; Ghosal, S.; Liebow, C.; Nagy, A.; Schally, A. A. W.; Prasad, P. N. *Proc. Natl. Acad. Sci.* **1999**, *96*, 11081.
- (8) Krebs, L. J.; Wang, X.; Pudavar, H. E.; Bergey, E. J.; Schally, A. A. W.; Nagy, A.; Prasad, P. N.; Liebow, C. *Cancer Res.* **2000**, *12* (9), 2632.

- (9) Bhawalkar, J. D.; Kumar, N. D.; Zhao, C. F.; Prasad, P. N. *J. Clin. Laser Med. Surg.* **1997**, *15*, 201.
- (10) Wachter, E. A.; Partridge, W. P.; Fish, W. G.; Dees, H. C.; Petersen, M. G. *Proc. SPIE-Int. Soc. Opt. Eng.* **1998**, *3269*, 68.
- (11) Joshi, M.; Pudavar, H. E.; Swiatkiewicz, J.; Prasad, P. N.; Reinhardt, B. A. *Appl. Phys. Lett.* **1999**, *74* (2).
- (12) Belfield, K. D.; Ren, X.; Hagan, D. J.; Van Stryland, E. W.; Dubikovsky, V.; Miesak, E. *J. Polym. Mater. Sci. Eng.* **1999**, *81*, 79.
- (13) Reinhardt, B. A.; Brott, L. L.; Clarson, S. J.; Dillard, A. G.; Bhatt, J. C.; Kannan, R.; Yuan, L.; He, G. S.; Prasad, P. N. *Chem. Mater.* **1998**, *10*, 1863.
- (14) Albota, M.; Beljonne, D.; Bredas, J.-L.; Ehrlich, J. E.; Fu, J.-Y.; Heikal, A. A.; Hess, S. E.; Kogej, T.; Levin, M. D.; Marder, S. R.; McCord-Maughon, D.; Perry, J. W.; Rockel, H.; Rumi, M.; Subramaniam, G.; Webb, W. W.; Wu, X.-L.; Xu, C. *Science* **1998**, *281*, 1653.
- (15) Spangler, C. W. *J. Mater. Chem.* **1999**, *9*, 2013.
- (16) Kim, O.-K.; Lee, K.-S.; Woo, H. Y.; Kim, K.-S.; He, G. S.; Swiatkiewicz, J.; Prasad, P. N. *Chem. Mater.* **2000**, *12*, 285.
- (17) Baur, J. W.; Alexander Jr., M. D.; Banach, M.; Denny, L. R.; Reinhardt, B. A.; Vaia, R. A.; Fleitz, P. A.; Kirkpatrick, S. M. *Chem. Mater.* **1999**, *11*, 2899.
- (18) Belfield, K. D.; Hagan, D. J.; Stryland, E. V.; Schafer, K. J.; Negres, R. A. *Org. Lett.* **1999**, *10*, 1576.
- (19) Ventelon, L.; Moreaux, L.; Martz, J.; Blanchard-Desce, M. *Chem. Commun.* **1999**, 2055.

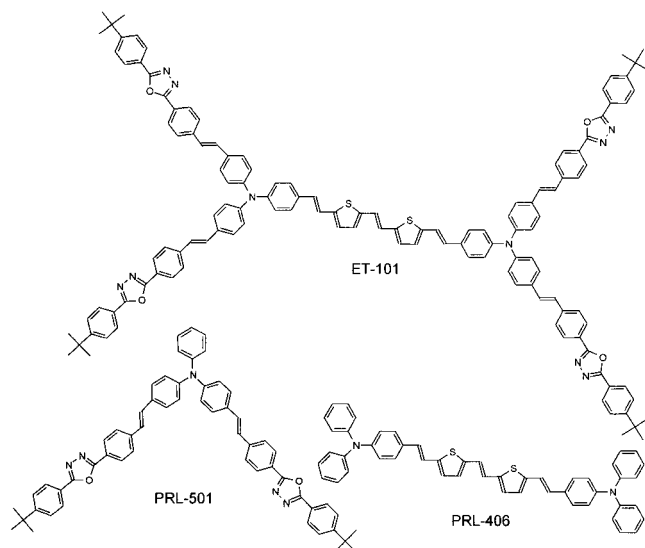


Figure 1. Chemical structures of **PRL-406**, **PRL-501**, and **ET-101**.

studied to understand design criteria for producing structures with enhanced two-photon activity.¹⁴

Recently, we reported two-photon properties of multi-branched structures, which involve linkage of asymmetrically substituted two- or three-chromophore units through an amino group.²⁰ In this paper we report the synthesis and optical properties of a new multibranching structure, bis(5-[4-{*N,N*-di(4-[4-{5-(4-*tert*-butylphenyl)-1,3,4-oxadiazol-2-yl}styryl]phenyl)amino}styryl]thien-2-yl)ethenylene (abbreviated as **ET-101**), which consists of distinct segments acting as chromophores. The **ET-101** molecular structure is shown in Figure 1 along with the structures of the **PRL-406** and **PRL-501** dyes related to the bridging segment and the branch (arm) segments of **ET-101**, respectively. The full names are bis(5-[4-{*N,N*-diphenylamino}styryl]thien-2-yl)ethenylene for **PRL-406** and (*N,N*-di[4-{4-(5-[4-*tert*-butylphenyl]-1,3,4-oxadiazol-2-yl)styryl]phenyl)amino}benzene for **PRL-501**, respectively.

The distinct chromophore segments of the **ET-101** molecule are as follows: The **PRL-501**-like and the **PRL-406**-like are different in the absorption and emission properties as expected from the analysis of the spectra of pure compounds **PRL-501** and **PRL-406**. The former is a higher-energy band gap green light emitting dye, and the latter is a red light emitting dye with a lower-energy band gap. We can expect that these two chromophores built into the **ET-101** molecule by sharing two triphenylamine groups would promote effective intrasystem excitation transport and conversion from the higher-energy state to the lower one. The two-photon absorption is measured using femtosecond pulse excitation for cross-section evaluation at the wavelength of 790 nm. This pulse excitation is also chosen as the two-photon excitation for time-resolved pump-probe experiments with an aim to reveal electronic states involved in early stages of the exciton dynamics. In the shorter-wavelength (620–780 nm) region two-photon absorption of the multibranching compound (**ET-101**) is compared

with a 2:1 stoichiometric mixture of **PRL-501** and **PRL-406** in order to wavelength dependence of two-photon excitation efficiency.

Experimental Section

Materials. Triphenylamine, phosphorus oxychloride, hydrochloride, tetrakis(triphenylphosphine)palladium(0), tri-*o*-tolylphosphine, tetrabutylammonium tribromide, 4-*tert*-butylbenzoyl chloride, *p*-toluic hydrazide, potassium *tert*-butoxide, iodomethane, triethyl phosphite, butyllithium, triethylamine, tetrahydrofuran, sodium borohydride, and palladium acetate were purchased from Aldrich Chemical Co. and used without further purification. The silica gel (100–200 mesh) used in column chromatography was purchased from Fisher Chemicals.

Synthesis. 4-[*N,N*-Di(4-bromophenyl)amino]benzaldehyde (**2**). (Diphenylamino)benzaldehyde (**1**)²¹ (10 g; 23 mmol) was dissolved in 250 mL of methylene chloride, and bromine (9.5 g; 53 mmol) was slowly added with vigorous stirring at room temperature. The mixture was stirred at room temperature for 6 h and poured into large excess 1 M sodium hydroxide solution. The methylene chloride layer was then separated. After methylene chloride was removed by distillation using a rotary evaporator, the residue was thoroughly washed with methanol. The product thus obtained (yield 12.7 g, 63%; mp = 168 °C) was pure enough to be utilized in the next step. Anal. Calcd (%) for C₁₉H₁₃Br₂NO: C, 52.93; H, 3.39; N, 3.71; Found: C, 52.74; H, 3.52; N, 4.02. ¹H NMR (300 MHz, CDCl₃, ppm): δ 7.03 (m, *J* = 6.6 Hz, 6H, Ar), 7.45 (d, *J* = 8.7 Hz, 4H, Ar), 7.72 (d, *J* = 8.7 Hz, 2H, Ar), 9.84 (s, H, -CHO).

4-(*N,N*-Bis[4-{4-(5-[4-*tert*-butylphenyl]-1,3,4-oxadiazol-2-yl)styryl]phenyl)amino]benzaldehyde (**4**). The 4-[*N,N*-di(4-bromophenyl)amino]benzaldehyde (**2**) (5 g; 12 mmol), tri-*o*-tolylphosphine (0.85 g; 26 mmol), triethylamine (6 mL), CH₃CN (6 mL), vinyloxadiazole compound (**3**)²⁰ (7.76 g; 26 mmol), and palladium(II) acetate (0.1 g; 0.46 mmol) were added to a pressure tube with plunger valves and thermowells equipped with a magnetic stirrer. The solution was heated at reflux by means of an oil bath for 24 h. After the mixture was cooled to room temperature, the mixture was poured with vigorous stirring into 200 mL of methanol. The precipitate formed was collected on a filter and washed thoroughly with methanol. The crude product was recrystallized from methanol. The yield was 5.88 g (56%; mp = 297 °C). Anal. Calcd (%) for C₅₉H₅₁N₅O₃: C, 80.70; H, 5.85; N, 7.98. Found: C, 81.12; H, 5.74; N, 8.22. ¹H NMR (300 MHz, CDCl₃, ppm): δ 1.38 (s, 18H, -C(CH₃)₃), 7.02 (d, *J* = 9.9 Hz, 4H, CH=CH), 7.03–8.17 (m, 28H, Ar), 9.81 (s, H, -CHO).

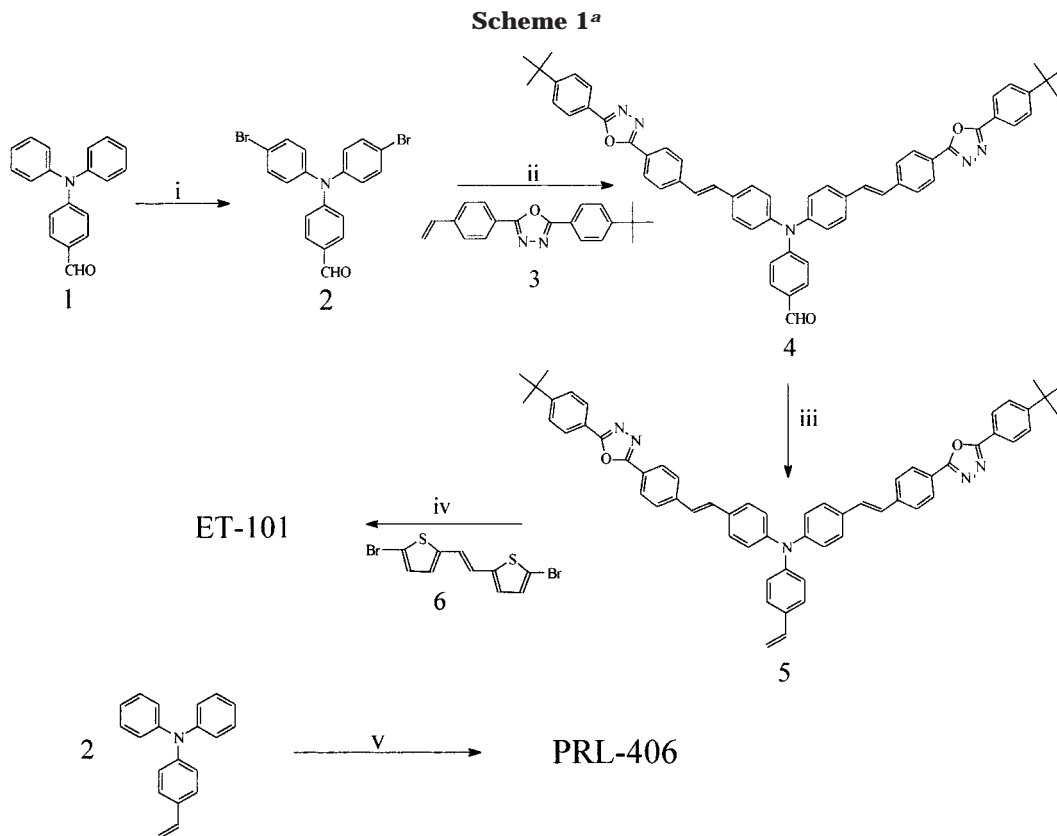
4-(*N,N*-Bis[4-{4-(5-[4-*tert*-butylphenyl]-1,3,4-oxadiazol-2-yl)styryl]phenyl)amino]styrene (**5**). Compound **4** (5 g; 5.7 mmol) and methyl phosphonium iodide (4.4 g; 11 mmol) were dissolved in 150 mL of tetrahydrofuran (THF). To this solution was added 1.4 g (44 mmol) of sodium hydride as strong base at room temperature. The mixture was refluxed for 6 h under a nitrogen atmosphere and then poured into excess distilled water. The precipitate was recrystallized from methanol. The product yield was 4.2 g (84%; mp = 264 °C). Anal. Calcd (%) for C₆₀H₅₃N₅O₂: C, 82.23; H, 6.10; N, 7.99. Found: C, 82.51; H, 5.94; N, 8.76. ¹H NMR (300 MHz, CDCl₃, ppm): δ 1.38 (s, 18H, -C(CH₃)₃), 5.21 (d, *J* = 11.9 Hz, 2H, -CH=CH₂), 5.65 (d, *J* = 17.1 Hz, H, -CH=CH₂), 7.02 (d, *J* = 8.6 Hz, 4H, CH=CH), 7.06–8.14 (m, 28H, Ar).

Bis(5-[4-{*N,N*-di(4-[4-{5-(4-*tert*-butylphenyl)-1,3,4-oxadiazol-2-yl}styryl]phenyl)amino}styryl]thien-2-yl)ethenylene (**ET-101**). The vinyl compound **5** (1 g; 1.1 mmol), tri-*o*-tolylphosphine (0.034 g; 0.11 mmol), triethylamine (2 mL), CH₃CN (4 mL), di-[2-(5-bromothieryl)]ethenylene (**6**)²² (0.16 g; 0.45 mmol), and palladium(II) acetate (0.004 g; 18 μmol) were added to a

(21) Tew, G. N.; Pralle, M. U.; Stupp, S. I. *Angew. Chem., Int. Ed. Engl.* **2000**, *39*, 517.

(22) Bouachrine, M.; Lere-porte, J.-P.; Moreau, J. J. E.; Torreilles, C. *J. Chim. Phys.-Chim. Biol.* **1998**, *95* (6), 1176.

(20) Chung, S.-J.; Kim, K.-S.; Lin, T.-C.; He, G. S.; Swiatkiewicz, J.; Prasad, P. N. *J. Phys. Chem. B* **1999**, *103*, 10741.



^a (i) Br₂, CH₂Cl₂, room temperature, 63%; (ii) Pd(OAc)₂, P(*o*-tolyl)₃, Et₃N/CH₃CN, 90 °C, 24 h, 56%; (iii) NaH, CH₃I-PPh₃⁺, THF, 60 °C, 6 h, 84%; (iv) Pd(OAc)₂, P(*o*-tolyl)₃, Et₃N/CH₃CN, 90 °C, 48 h, 32%; (v) Pd(OAc)₂, P(*o*-tolyl)₃, Et₃N/CH₃CN, 90 °C, 24 h, 54%.

pressure tube with plunger valves and thermowells equipped with a magnetic stirrer. The solution was heated and refluxed for 48 h. After the mixture was cooled to room temperature, the mixture was poured with vigorous stirring into 200 mL of acetone. The precipitate formed was collected on a filter and washed thoroughly with acetone. The crude product was purified by column chromatography using silica gel and a 70/30 hexane/methylene chloride mixture as eluent to afford a dark red solid in 32% yield (mp = 296–298 °C). Anal. Calcd (%) for C₁₃₀H₁₁₀N₁₀O₄S₂: C, 80.46; H, 5.71; N, 7.22; S, 3.30. Found: C, 81.62; H, 5.69; N, 6.89; S, 3.44. ¹H NMR (300 MHz, CDCl₃, ppm): δ 1.38 (s, 18H, -C(CH₃)₃), 6.87–6.96 (m, broad, 14H, CH=CH), 7.0–8.31 (m, 78H, Ar). FAB-MS: *m/z*: 1941.6 [M + H].

Bis[5-[4-{*N,N*-diphenylamino}styryl]thien-2-yl]ethynylene (PRL-406). (Diphenylamino)styrene (**1**) (3 g; 11 mmol), tri-*o*-tolylphosphine (0.33 g; 1.1 mmol), triethylamine (4 mL), CH₃CN (8 mL), bis[2-(5-bromothieryl)]ethynylene (**6**) (0.48 g; 1.4 mmol), and palladium(II) acetate (0.012 g; 53 μmol) were added to a pressure tube with plunger valves and thermowells equipped with a magnetic stirrer. The solution was heated at reflux by means of an oil bath for 24 h. After the mixture was cooled to room temperature, the mixture was poured with vigorous stirring into 200 mL of methanol. The precipitate formed was collected on a filter and washed thoroughly with methanol. The crude product was purified by column chromatography using silica gel and hexane as eluent to afford a dark red solid in 54% yield (mp = 255 °C). Anal. Calcd (%) for C₅₀H₃₈N₂S₂: C, 82.16; H, 5.24; N, 3.83; S, 8.77. Found: C, 82.72; H, 5.31; N, 4.02; S, 7.97. ¹H NMR (400 MHz, CDCl₃, ppm): δ 6.87 (d, *J* = 4.8 Hz, 2H, CH=CH), 6.90 (d, *J* = 4.8 Hz, 2H, CH=CH), 6.96 (d, *J* = 4.8 Hz, 2H, CH=CH), 7.03–7.57 (m, 28H, Ar), 7.58 (d, *J* = 8.4 Hz, 2H, Ar), 8.19 (d, *J* = 8.4 Hz, 2H, Ar). FAB-MS: *m/z*: 731.9 [M + H].

Characterizations. Linear absorption spectra were recorded on an automatic spectrophotometer (Shimadzu, UV-3101PC) for diluted solutions, *c* = 1 × 10⁻⁴ M in THF using a 1 mm path length cell. The fluorescence studies were con-

ducted with 1 × 10⁻³ M solutions in THF using a Shimadzu, RF50000U spectrofluorimeter.

The Z-scan apparatus utilizing femtosecond pulses and the arrangement of the pump-probe experiment are described elsewhere.²³ The data analysis follows the method also described previously.²³ The laser system based on titanium:sapphire oscillator generated a train (93 MHz) of 80 fs pulses at the central wavelength of 790 nm. Selected pulses were amplified in a titanium:sapphire regenerative amplifier using a chirp-pulse amplification scheme. The final pulse energy was about 200 μJ, but only a small fraction of this energy (below 1 μJ) was used in experiments at 790 nm. The pulse length of the amplified pulse was checked with an autocorrelator, and it was typically about 130 fs.

Full pulse energy (200 μJ) was used to pump a transient optical parametric generator/amplifier (TOPG/OPA) to obtain signal pulses in the 1.2–1.6 μm wavelength range. These pulses were frequency doubled in order to obtain femtosecond pulses in the wavelength range of 600–780 nm. Two β-barium borate (BBO) crystals, both of the 4 × 4 × 4 mm size, were used for type II and type I second-order interactions and were used for TOPG/OPA and second harmonic generation, respectively. The SHG output was about 0.5 μJ/pulse and was used in the Z-scan experiment at selected wavelengths.

Results and Discussion

Synthesis. The synthetic route to the multibranch two-photon chromophore (ET-101) and PRL-406 are shown in Scheme 1. Compound **4** was prepared from the vinyloxadiazole compound (**3**)²⁰ and [bis(bromophenyl)amino]benzaldehyde (**2**) under palladium-catalyzed Heck conditions²⁴ with 56% yield. The aldehyde group

(23) Swiatkiewicz, J.; Prasad, P. N.; Reinhardt, B. A. *Opt. Commun.* **1998**, *157*, 135.

(24) Dieck, H. A.; Heck, R. F. *J. Am. Chem. Soc.* **1974**, *96*, 1133.

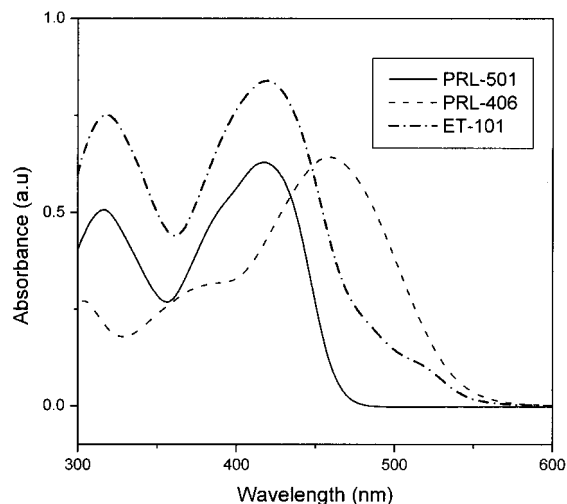


Figure 2. Absorption spectra of **PRL-406**, **PRL-501**, and **ET-101** solutions in THF. Concentration = 10^{-4} M.

in compound **4** was converted to the vinylene group by Wittig reaction²⁵ with methyl phosphonium iodide in the presence of NaH as a base with 84% yield. The resulting compound (**ET-101**), a multibranching two-photon chromophore, was obtained by the reaction of the vinyl compound **5** with the bis(bromothieryl)ethynylene compound **6**²² via Heck coupling with 32% yield. **PRL-406** was synthesized from (diphenylamino)styrene and bis(bromothieryl)ethynylene compound **6** via Heck coupling with 54% yield, and **PRL-501** was prepared in 47% yield using a previously published procedure.²⁰ All compounds were purified by column chromatography and recrystallization and confirmed by ¹H NMR, electronic spectra and elemental analysis. The pure final chromophores, **ET-101**, **PRL-406**, and **PRL-501**, are soluble in 1,1,2,2-tetrachloroethane, chloroform, and THF. **ET-101** and **PRL-406** are very dark red in color, and **PRL-501** is yellow-green in the solid state, respectively.

Linear Optical Properties of Chromophore Solutions. The one-photon absorption spectra of the **PRL-406**, **PRL-501**, and **ET-101** in THF are shown in Figure 2. The absorption band at about 300–320 nm is assigned to absorption of the phenylene ring, whereas the longer wavelength region absorption band is attributed to a charge-transfer band of the molecules.^{26,27} The maximum peaks of one photon absorption corresponding to the CT bands are at 457 nm for **PRL-406** and at 417 nm for **PRL-501**.²⁰ The strong absorption band for **ET-101** at about 420 nm is attributed to the higher-energy band gap moieties (**PRL-501**-like). The maximum molar extinction coefficients of the three chromophores are 8.40×10^5 , 6.42×10^5 , and 6.30×10^5 cm⁻¹ M⁻¹ for **ET-101**, **PRL-406**, and **PRL-501**, respectively. The **PRL-406**-like absorption band appears in the **ET-101**, as a weak shoulder in the 470–550 nm region. The absorption spectra shown in Figure 2 were measured for samples of equal concentrations (10^{-4} M). It is evident from the absorption peak values that the molar

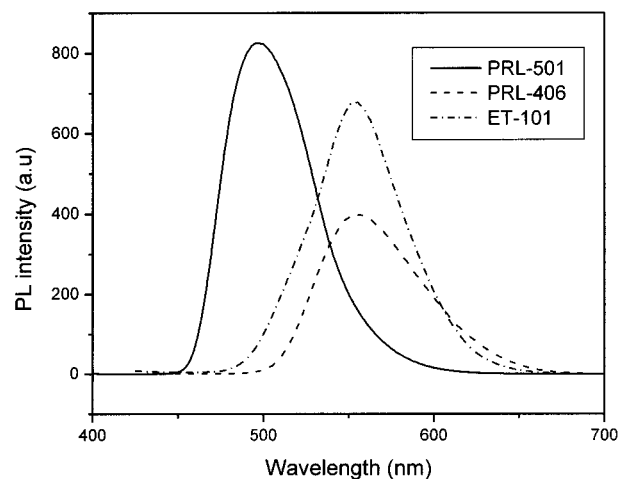


Figure 3. One-photon excited emission spectra of **PRL-406**, **PRL-501**, and **ET-101** solutions in THF. Concentration = 10^{-3} M.

extinction coefficient of **ET-101** is smaller than that expected if the chromophore groups would be effectively separated and noninteracting. The absorbance spectrum in the latter case should be a simple superposition of the component spectra and with about twice as large absorbance as derived from the **PRL-501**-like unit, which is not what is observed. The apparent hypochromic effect (the reduction of the oscillator strength) indicates a weak coupling between the different chromophore segments.

The emission spectra obtained using the same excitation wavelength of 400 nm for all three compounds are shown in Figure 3. The fluorescence of **PRL-501** is strong, in the green region, with a peak at 497 nm, but **PRL-406** exhibits a weak emission at 554 nm. However, the one-photon emission spectrum of **ET-101**, obtained for the excitation wavelength of 400 nm, shows only a strong emission band at about 552 nm. The strong emission band at about 552 nm is considered to be the emissions from the lower energy band gap bridging unit moiety (**PRL-406**-like) of **ET-101**. No emission from the higher energy band gap of the arm segments is obtained, indicating an efficient energy transfer from the arms (**PRL-501**-like) to the bridge segment (**PRL-406**-like). Absorbance at 400 nm of **ET-101** is at the peak associated with a similarly located electronic band in **PRL-501**. However, the emission is exclusively observed from the lowest electronic level which belongs to the central bridging segment. This level is formed with a main contribution of the **PRL-406**-like chromophore segment. The lack of arm's green emission in **ET-101** dissolved in solution also suggests a facile excitation migration from the outer arms to the central bridging unit. The luminescence quantum yields of the chromophores for the solutions of 1.0×10^{-4} mol/L are 0.21, 0.03, and 0.57 for **ET-101**, **PRL-406**, and **PRL-501**, respectively. Even though the luminescence quantum yield of **ET-101** showing only a strong emission from the lower energy band gap bridging unit moiety is lower than **PRL-501**, it is much higher than that of **PRL-406**. Such an increase in the quantum yield indicates an efficient excitation through energy transfer from the arms (**PRL-501**-like) to the bridge segment (**PRL-406**-like). It should be noted that in dilute solution only

(25) Maercker, A. *Org. React.* **1965**, *14*, 270.

(26) Gruen, H.; Gawraner, H. *J. Phys. Chem.* **1989**, *93*, 7144.

(27) Beljonne, D.; Bredas, J. L.; Cha, M.; Torruellas, W. E.; Stegeman, G. I.; Hofstraat, J. W.; Horshuis, W. H. G.; Mohlmann, G. *R. J. Chem. Phys.* **1995**, *103*, 7834.

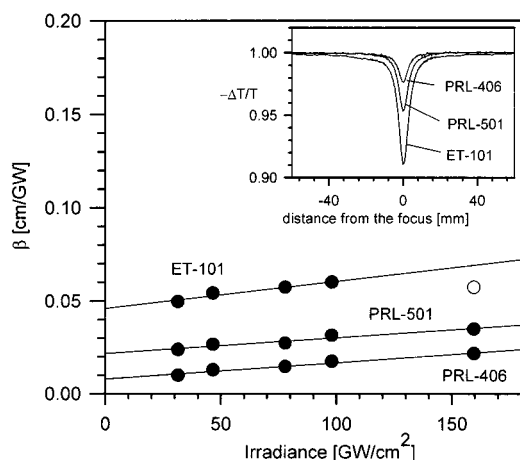


Figure 4. Z-scan trace (insert) and dependence of nonlinear absorption coefficient (β) on irradiance for the **PRL-406**, **PRL-501**, and **ET-101** of the equal concentration solutions in THF (5×10^{-3} M).

intrachain exciton migration and trapping occurs because of the separation between molecules.²⁸

Nonlinear Optical Properties of Chromophore Solutions. The TPA cross-section (σ) values were determined from experimentally measured two-photon absorption coefficient (β): $\sigma = h\nu\beta/N_0 = 10^3 h\nu\beta/N_A C$, where N_0 and N_A are the number density of assumed absorptive centers and the Avogadro number, respectively, and C is the solute molar concentration.

The β values of the three chromophores in THF solution were measured by the femtosecond Z-scan technique.²³ A typical signal trace for each compound dissolved in tetrahydrofuran at the same concentration is shown in the insert of Figure 4. For these experiments, the average pulse length was 131 fs, and the peak irradiance at the focal point was 48 GW/cm² at a wavelength of 790 nm. The repetition rate was kept at 1000 Hz, and under this condition no cumulative effect from slow photophysical or photochemical processes was observed. The depth of the valley in the Z-scan is proportional to the nonlinear absorption coefficient of the respective samples, and, for their equal concentration, they are proportional to the effective two-photon cross-section.

In a series of Z-scan experiments, but with variable peak irradiance, a power dependence of the nonlinear absorption is observed and is shown in Figure 4. A monotonic linear increase of β for increasing irradiance is indicative of excited-state linear absorption.²³ Time-resolved pump-probe experiments confirm the role of linear absorption of the two-photon excited states for all three compounds. The transients shown in Figure 5 reveal substantial two-photon excited-state absorption (later called an induced absorbance for brevity). It is clearly observed after the peak associated with a coherent effect caused by the pump and probe pulse temporal overlap. Induced absorbance prior to the pump pulse, in the negative time delay, is practically zero. Therefore, the induced absorbance must rise during the excitation pulse period and may contribute to the irradiance effects on the effective β observed in our Z-scan experiments.

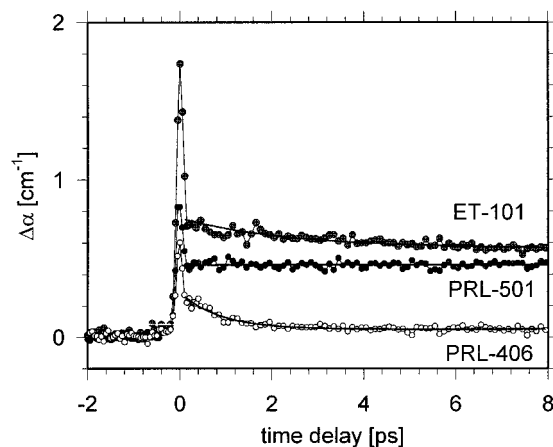


Figure 5. Transient two-photon induced absorption in the femtosecond pump-probe experiment. The continuous line along the delayed signal is the best fit for the data with a one-exponent relaxation.

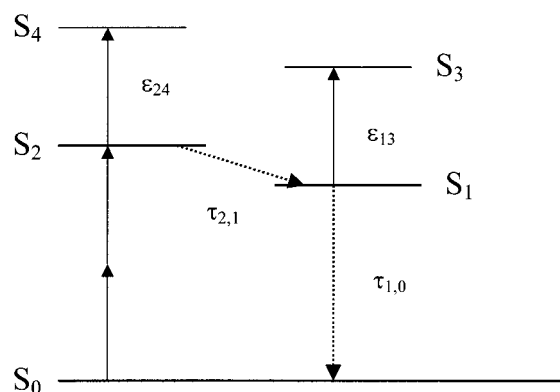


Figure 6. Proposed energy levels schematics.

After the pump pulse, the two-photon induced absorbance decays very fast for the **PRL-406** solution ($\tau = 0.9$ ps) and slower for the **ET-101** ($\tau = 9$ ps). These relaxations may correspond to the transition from a “hot” electronic state, with symmetry allowing for two-photon excitation, to a lower-energy electronic state relaxed to a different geometry from which a radiative transition to the ground state is possible (lowest singlet). The observed difference in decay rate can tentatively be associated with a more complex multistep relaxation process including for the **ET-101** molecule. We can construct a tentative energy level schematic for the molecules discussed here which is shown in Figure 6. We assume the fast transient occurs within the same parity manifold and all levels are marked as the singlets ($S_0 - S_4$). The two-photon absorption event populates the S_2 singlet which for **ET-101** is primarily localized in the arms segments. The S_4 singlet, located above the S_2 in the energy scale in Figure 6, can be reached from the ground state (S_0) through a three-photon excitation or by a one-photon absorption from the S_2 excited state. The probability of the latter process is expressed by an extinction coefficient ϵ_{24} . Both processes reveal themselves in the femtosecond Z-scan experiment as a power dependent effective two-photon cross-section.²³ Time-resolved experiments indicate that, at least for the **ET-101** and **PRL-406** samples, the S_2 singlet relaxes to the lowest singlet level S_1 in a few picoseconds. For **ET-101** this is the emissive state associated with the

(28) Lee, J.-I.; Zyung, T.; Miller, R. M.; Kim, Y. H.; Jeoung, S. C.; Kim, D. J. *Mater. Chem.* **2000**, *10*, 1547.

bridging segment. The emissive state also exhibits linear absorption (ϵ_{13}), and it has a relatively long lifetime ($\tau_{10} \sim \text{ns}$) dictated by the dynamics of the radiative process, the fluorescence. Considering the delayed linear absorption as shown in Figure 5, the transition from the S_2 to the S_1 state can only be observed in the form of an absorption transient if the parameters ϵ_{24} and ϵ_{13} are different. This is true for the **ET-101** and **PRL-406** samples, whereas for the **PRL-501** the difference $\epsilon_{24} - \epsilon_{13}$ is probably too small and the delayed linear absorption appears constant in Figure 5. The energy schematics and the sequence of events given here provide only a tentative model. The assignment of the S_1 state as the lowest emissive singlet state needs to be established by further study of the photoluminescence dynamics. The origin and the character of the S_3 and S_4 states also need to be established.

Linear extrapolation of the nonlinear absorption coefficient measured for various irradiance (see Figure 4) provides data for calculating the true electronic two-photon absorption cross-sections of the **ET-101**, **PRL-406**, and **PRL-501** molecules. The respective values of σ_{TPA} are 1.52×10^{-20} , 0.26×10^{-20} , and $0.73 \times 10^{-20} \text{ cm}^4/\text{GW}$. The data clearly indicate that the contribution of the **PRL-501** chromophore dominates the two-photon absorption cross-section of the **ET-101** dye at 790 nm. Assuming that the σ coefficient of **ET-101** can be represented as a sum of the respective components, we can estimate the contribution from the **PRL-501** chromophore as $(2\sigma_{\text{PRL501}}/\sigma_{\text{ET101}}) = 0.96$ and, from the **PRL-406** as $(\sigma_{\text{PRL406}}/\sigma_{\text{ET101}}) = 0.17$, for the excitation wavelength of 790 nm. These contributions are approximate values, since the **PRL-501** molecule and the **PRL-406** molecule are larger size chromophores than the respective constituent units of the **ET-101**. Considering also an experimental error of 10–15%, we conclude that there is no significant enhancement of two-photon absorption at 790 nm for the **ET-101** dye, compared to those from the constituent segments.

Having measured the Z -scan profiles at several wavelengths, shorter than 790 nm, we can compare the nonlinear absorption effects for the dyes in the wavelength range of 620–790 nm. The experiment results were not corrected for the slight changes of beam divergence of the SHG output during the wavelength scan, so it prevented us from obtaining the two-photon absorption spectra. However, we can discuss relative values obtained for a specific wavelength, as the Z -scan for each dye was registered under the same conditions: the wavelength, the pulse length, pulse energy, and the beam propagation.

For a specific wavelength the Z -scan valley depth (S) was recorded for each dye and the ratio $((S_{\text{ET101}})/(2S_{\text{PRL501}} + S_{\text{PRL406}}))$ was calculated. This ratio represents the effectiveness of the **ET-101** dye as compared to a stoichiometric mixture (2:1) of the **PRL-501** and **PRL-406** dyes in relation to their nonlinear absorption. We involve here a summation concept of the two-photon cross-sections for the components. The results are shown in Figure 7. The **ET-101** dye, apparently is a less efficient two-photon absorber than the equivalent stoichiometric mixture of the **PRL-501** and **PRL-406**. The difference spans from 35 to 80% compared to the mixture, depending on the wavelength. This difference

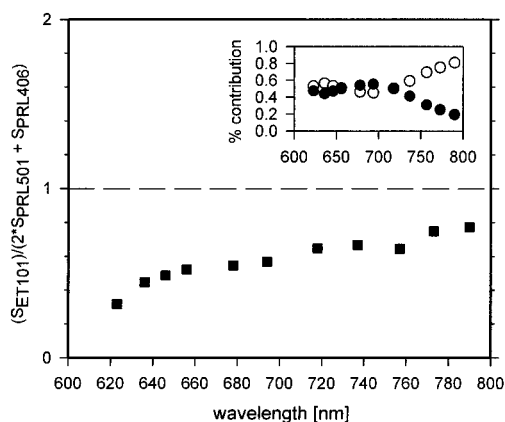


Figure 7. Relative two-photon cross-section of the **ET-101** dye compared to a stoichiometric mixture of the **PRL-406** and **PRL-501** dyes at various wavelength. Insert: Open circles, calculated contribution of the **PRL-501**; solid circles, contribution of the **PRL-406** to the nonlinear absorption at their 2:1 stoichiometric mixture.

reduces monotonically as the excitation wavelength approaches 790 nm. It is not clear whether the **ET-101** dye is less efficient or the mixture is relatively more effective at shorter wavelengths. An interesting observation is shown in the insert of Figure 7. It illustrates the calculated contributions from the component dyes relative to the nonlinear absorption of the mixture. In the short wavelength range (600–720 nm), the contributions from the both dyes are almost equal; however, in the longer wavelength range (>720 nm), the contribution from **PRL-501** steeply increases. The **PRL-501** component is contributing overwhelmingly in the spectral range > 720 nm in the **ET-101** dye as the dye solution and the stoichiometric mixture behave similarly for this range.

Conclusion

We have synthesized a new multibranch compound (**ET-101**) with a molecule consisting of two types of chromophore groups of different electronic excited-state energies. This compound exhibits a very effective intramolecular energy conversion between the states derived from the constituents and a large two-photon absorption cross-section. Comparing its two-photon absorption cross-section with a stoichiometric mixture of the two dyes closely resembling the chromophore groups (**PRL-501**, **PRL-406**), we did not observe any cooperative enhancement of two-photon absorption in **ET-101** at an excitation wavelength of 790 nm. Moreover, the **ET-101** dye is increasingly less effective than the mixture at shorter wavelengths.

Acknowledgment. This work was supported by the Air Force Office of Scientific Research, Directorate of Chemistry and Life Sciences, through Contract F496200010064.

Supporting Information Available: Figures showing excitation spectra and fluorescence decay behavior and text describing the measurement method of the quantum yield for **PRL-501**, **PRL-406**, and **ET-101** in solution (PDF). This material is available free of charge via the Internet at <http://pubs.acs.org>.